

Oxidative decarbonylation of $\text{Mo}(\text{CO})_6$ with $[-\text{Se}(\text{Se})\text{P}(\text{O}i\text{-Pr})_2]_2$ generates the mixed-valent tetranuclear cluster $\text{Mo}_4(\mu_3\text{-Se})_4[\text{Se}_2\text{P}(\text{O}i\text{-Pr})_2]_6$ and a cationic trinuclear cluster $[\text{Mo}_3(\mu_3\text{-Se})(\mu_2\text{-Se}_2)_3\{\text{Se}_2\text{P}(\text{O}i\text{-Pr})_2\}_3]^+$

C.W. Liu^{a,*}, Ching-Shiang Fang^a, Chin-Wei Chuang^a, Tarlok S. Lobana^{a,1},
Ben-Jie Liaw^a, Ju-Chun Wang^b

^a Department of Chemistry, National Dong Hwa University, Hualien 974, Taiwan

^b Department of Chemistry, Soochow University, Taipei 111, Taiwan

Received 7 October 2006; received in revised form 19 December 2006; accepted 22 December 2006

Available online 9 January 2007

Abstract

Oxidative decarbonylation of $\text{Mo}(\text{CO})_6$ with $[-\text{Se}(\text{Se})\text{P}(\text{O}i\text{-Pr})_2]_2$ yielded a novel tetranuclear, mixed-valent ($\text{Mo}^{\text{III/IV}}$) $\text{Mo}_4(\mu_3\text{-Se})_4[\text{Se}_2\text{P}(\text{O}i\text{-Pr})_2]_6$ cluster **1** (dark brown), and a trinuclear, $[\text{Mo}_3(\mu_3\text{-Se})(\mu_2\text{-Se}_2)_3\{\text{Se}_2\text{P}(\text{O}i\text{-Pr})_2\}_3][\text{Se}_2\text{P}(\text{O}i\text{-Pr})_2]$ cluster **2a** (orange). The uncoordinated $\text{Se}_2\text{P}(\text{O}i\text{-Pr})_2$ anion of **2a** was replaced by halide anions to yield $[\text{Mo}_3(\mu_3\text{-Se})(\mu_2\text{-Se}_2)_3\{\text{Se}_2\text{P}(\text{O}i\text{-Pr})_2\}_3](\text{X})$ ($\text{X} = \text{Cl}$, **2b**; Br , **2c**; I , **2d**) via the anion exchange reactions. In cluster **1**, each Mo atom is bonded to two Se atoms from one chelating *dsep* (*dsep* = diselenophosphates) ligand, one Se from bridging *dsep* and to three, triply bridging $\mu_3\text{-Se}$ atoms with $\text{Mo}-\mu_3\text{-Se}$ bond distances, 2.4580–2.503 Å, and $\text{Mo}-(^1\eta\text{-Se})$ bond distances, 2.691–2.729 Å. The cyclic voltammogram of **1** reveals one quasi-reversible one-electron oxidation wave ($E_{1/2} = 0.67$ V), corresponding to the formation of the $\text{Mo}_4\text{Se}_4^{7+}$ state, and two quasi-reversible one-electron reduction waves ($E_{1/2} = -0.23$ and -1.09 V), suggesting the formation of $\text{Mo}_4\text{Se}_4^{5+}$ and $\text{Mo}_4\text{Se}_4^{4+}$ cores. In cluster cation, **2**, three Mo atoms form an equilateral triangle which is capped by a $\mu_3\text{-Se}^{2-}$ anion, and each Mo atom is further coordinated to two $\mu_2\text{-Se}_2^{2-}$ ligands and a chelated *dsep* ligand. Interestingly, clusters **2a–2d** exhibited unusual, intermolecular $\text{Se}\cdots\text{Se}$ interactions to produce infinite chains. All “sandwiched” halides are attached to three Se_{ax} atoms of one Mo_3 unit and one Se_{eq} atom of the neighboring unit in clusters **2b–2d** and these distances are far shorter than the sum of the van der Waals radii.

© 2007 Elsevier B.V. All rights reserved.

Keywords: Molybdenum; Diselenophosphates; $\text{Se}\cdots\text{Se}$ interactions; $\text{Se}\cdots\text{X}$ interactions; Oxidative decarbonylation

1. Introduction

The chemistry of chalcogenide-containing molybdenum clusters is gaining interest in view of their unusual electrical properties [1]. For example, the sulfur cluster core $[\text{Mo}_3(\mu_3\text{-S})(\mu_2\text{-S}_2)_3]^{4+}$ with outer dithiolate ligands has been used as single-component magnetic conductors.¹ The sulfur- and

selenium-based trinuclear cores $[\text{Mo}_3(\mu_3\text{-E})(\mu_2\text{-E}_2)_3]^{4+}$ ($\text{E} = \text{S}, \text{Se}$) have been studied broadly for their ligand chemistry [2–7]. Molybdenum also forms a cuboidal Mo_4Se_4 core, which unlike its sulfur analog has been little investigated for its ligand chemistry [2]; and only a few complexes such as, $[\text{Mo}_4(\mu_3\text{-Se})_4(\text{CN})_{12}]^{8-}$ [8], $[\text{Mo}_4(\mu_3\text{-Se})_4(\text{H}_2\text{O})_{12}]^{5+}$ [9], $[\text{Mo}_4(\mu_3\text{-Se})_4(\text{edta})_2]^{3-}$ [10], $[\text{Mo}_4(\mu_3\text{-Se})_4(\text{Cp-}i\text{-Pr})_4]$ [11], and $\text{Mo}_4(\mu_3\text{-Se})_4[\text{S}_2\text{P}(\text{OEt})_2]_6$ [7b] are known. The cubane-type structures have been shown to possess optical limiting effects [12].

We have been interested in the coordination chemistry of diselenophosphates (*dsep*), $\text{Se}_2\text{P}(\text{OR})_2^-$, possessing Se

* Corresponding author. Fax: +886 3 8633570.

E-mail address: chenwei@mail.ndhu.edu.tw (C.W. Liu).

¹ Current address: Department of Chemistry, Guru Nanak Dev University, Amritsar 143005, India.

donor atoms, which have exhibited unusual selenium transfer ability in the formation of several Cu^{I} , Ag^{I} and Zn^{II} clusters: $[\text{Cu}_8(\mu_8\text{-Se})\{\text{Se}_2\text{P}(\text{OR})_2\}_6]$ ($\text{R} = \text{Et}, \text{Pr}, i\text{-Pr}$), $[\text{Cu}_{11}(\mu_9\text{-Se})(\mu_3\text{-X})_3\{\text{Se}_2\text{P}(\text{OR})_2\}_6]$ ($\text{X} = \text{Br}, \text{I}, \text{R} = \text{Et}, \text{Pr}, i\text{-Pr}$), $[\text{Ag}_8(\mu_8\text{-Se})\{\text{Se}_2\text{P}(\text{O}i\text{-Pr})_2\}_6]$, $[\text{Ag}_{10}(\mu_{10}\text{-Se})\{\text{Se}_2\text{P}(\text{OEt})_2\}_6]$, $[\text{Ag}_{11}(\mu_9\text{-Se})(\mu_3\text{-I})_3\{\text{Se}_2\text{P}(\text{OR})_2\}_6]$ ($\text{R} = \text{Et}, i\text{-Pr}, \text{sec-Bu}$) and $[\text{Zn}(\mu_4\text{-Se})\{\text{Se}_2\text{P}(\text{OR})_2\}_6]$ ($\text{R} = \text{Et}, \text{Pr}, i\text{-Pr}$) [13]. In all these clusters, the origin of $\mu_n\text{-Se}$ ($n = 4, 8, 9$ and 10) is the *dsep* ligand itself, though the mechanism of its formation in the reaction mixture is not yet well-understood. In view of our interest to establish the generality of Se transfer property of *dsep* ligands, it was considered worthwhile to investigate molybdenum chemistry, owing to its importance highlighted above.

In this article, we report the synthesis of tetranuclear $\text{Mo}_4(\mu_3\text{-Se})_4[\text{Se}_2\text{P}(\text{O}i\text{-Pr})_2]_6$ (**1**) and trinuclear, cationic $[\text{Mo}_3(\mu_3\text{-Se})(\mu\text{-Se}_2)_3\{\text{Se}_2\text{P}(\text{O}i\text{-Pr})_2\}_3]^+$ (**2**) clusters bearing diselenophosphate ligands. There is no reported complex containing $[\text{Mo}_4(\mu_3\text{-Se})_4]$ cubane cores with outer selenium-donor ligands [7–11], and among recently reported clusters of dithiophosphates (dtp) with Mo and mixed metals (Mo/W), viz., $\text{Mo}_n\text{W}_m(\mu_3\text{-Se})_4[\text{S}_2\text{P}(\text{OEt})_2]_6$ ($n = 1\text{--}4$; $m = 4\text{--}n$), only the crystal structure of $\text{Mo}_4(\mu_3\text{-Se})_4[\text{S}_2\text{P}(\text{OEt})_2]_6$ is known [7b]. Intermolecular $\text{Se}\cdots\text{Se}$ interactions exist between the tri-molybdenum clusters in **2** to produce infinite chains. Furthermore, clusters **1** and **2** were obtained from the oxidative decarbonylation of $\text{Mo}(\text{CO})_6$ with $[-\text{Se}(\text{Se})\text{P}(\text{O}i\text{-Pr})_2]_2$, an oxidized form of the *dsep* ligand. To our knowledge, none of the metal diselenophosphato complexes has been synthesized via the utilization of $[-\text{Se}(\text{Se})\text{P}(\text{O}i\text{-Pr})_2]_2$ as the selenophosphate synthon [14].

2. Experimental

2.1. Materials and techniques

All chemicals and reagents obtained from commercial sources were purified/dried. Commercial CH_2Cl_2 and MeOH were distilled from P_4O_{10} and Mg, respectively. Ligands $[-\text{Se}(\text{Se})\text{P}(\text{O}i\text{-Pr})_2]_2$ were prepared by modified methods reported in the literature [15] and confirmed by elemental analysis, the single crystal X-ray diffraction study, and multinuclear NMR (^1H , ^{31}P and ^{77}Se). Hexane and diethyl ether were distilled from Na/K. All the reactions were performed in oven-dried Schlenk glassware by using standard inert-atmosphere techniques. NMR spectra were recorded on a Bruker AC-F200 or Advance-300 Fourier transform spectrometers. The $^{31}\text{P}\{^1\text{H}\}$ and $^{77}\text{Se}\{^1\text{H}\}$ NMR are referenced externally against 85% H_3PO_4 ($\delta = 0$) and PhSeSePh ($\delta = 463$ ppm), respectively. The elemental analyses (C, H) obtained by using a Perkin Elmer 2400 analyzer. Melting points were measured by using Fargo melting point apparatus, MP-2D. Positive ion FAB mass spectra were obtained from VG 70-250S mass spectrometer by using nitrobenzyl alcohol as the matrix. Electrochemical

measurements were carried out with a three-electrode setup, consisting of a platinum wire working, a saturated Ag/AgCl reference, and a platinum wire auxiliary electrode using a PST050 analytical voltammetry. The measurements were made at 25°C under a nitrogen atmosphere, and the data are uncorrected for junction potentials. Ferrocene was used as a standard showing the Fe(III)/Fe(II) couple at 0.45 V (vs Ag/AgCl) under similar experimental conditions in CH_2Cl_2 containing 0.1 M tetrabutylammonium hexafluorophosphate (TBAHP). The half-wave potential $E_{1/2}$ was set equal to $1/2(E_{\text{pa}} + E_{\text{pc}})$, where E_{pa} and E_{pc} are the anodic and cathodic peak potentials, respectively.

2.2. Synthesis of $[(i\text{-PrO})_2\text{P}(\text{Se})]_2(\text{Se})_2$

In a 50 mL Schlenk bottle was filled with $[\text{NH}_4][\text{Se}_2\text{P}(\text{O}i\text{-Pr})_2]$ (0.119 mg, 0.36 mmol) and FeCl_3 (59 mg, 0.36 mmol), then acetone (30 mL) was added to stir at 0°C . The solution color changed from black to orange-red within one minute; then a few white precipitates started to form along with red solution within 10 min of stirring. After filtration, the solvent was removed by rotavapor to obtain orange-red powders of $[-\text{Se}(\text{Se})\text{P}(\text{O}i\text{-Pr})_2]_2$ (106 mg, yield: 94%).

2.3. Syntheses of $[\text{Mo}_4(\mu_3\text{-Se})_4\{\text{Se}_2\text{P}(\text{O}i\text{-Pr})_2\}_6]$ (**1**) and $[\text{Mo}_3(\mu_3\text{-Se})(\mu_2\text{-Se}_2)_3\{\text{Se}_2\text{P}(\text{O}i\text{-Pr})_2\}_3][\text{Se}_2\text{P}(\text{O}i\text{-Pr})_2]$ (**2a**)

Treatment of $\text{Mo}(\text{CO})_6$ (0.150 g, 0.568 mmol) with $[-\text{Se}(\text{Se})\text{P}(\text{O}i\text{-Pr})_2]_2$ (0.500 g, 0.814 mmol) in 2:3 molar ratio in refluxing toluene (40 mL), for 4–5 h, followed by removal of solvent formed a solid residue, which after chromatographic separation (silica gel column, ethylacetate-*n*-hexane, 1:19, v/v) yielded two clusters: dark brown $[\text{Mo}_4(\mu_3\text{-Se})_4\{\text{Se}_2\text{P}(\text{O}i\text{-Pr})_2\}_6]$ (**1**) (yield: 0.175 g, 49%) and orange $[\text{Mo}_3(\mu_3\text{-Se})(\mu_2\text{-Se}_2)_3\{\text{Se}_2\text{P}(\text{O}i\text{-Pr})_2\}_3][\text{Se}_2\text{P}(\text{O}i\text{-Pr})_2]$ (**2a**) (yield: 0.100 g, 25%).

Compound 1: C, H analysis calcd for $\text{C}_{36}\text{H}_{84}\text{Mo}_4\text{P}_6\text{O}_{12}\text{Se}_{16}$: C 17.01; H 3.33. Found: C 17.26; H 3.31%. **1:** ^1H NMR (CDCl_3 , δ , ppm): 1.21 (d, 24H, CH_3), 1.31 (d, 24H, CH_3), 1.47 (d, 24H, CH_3), 4.45 (m, 4H, CH), 4.66 (m, 4H, CH), 5.04 (m, 4H, CH); ^{31}P NMR (CDCl_3 , δ , ppm): 120.7 (4P; $J_{\text{P-Se}}$ 614 Hz), 85.1 (2P; $J_{\text{P-Se}}$ 687 Hz); ^{77}Se NMR (CDCl_3 , δ , ppm): 126.3 {s, 4($\mu_3\text{-Se}$)}, 38.0 (d, 4Se, $J_{\text{P-Se}}$ 689), -35.1 (d, 8Se, $J_{\text{P-Se}}$ 610). Positive ion FAB-MS (Found/Calcd): m/z , 2542.0 (2540.7) [M^+], 2233.4 (2235.8) [(M-dsep) $^+$], 1926.5 (1928.9) [(M-2dsep) $^+$]. mp: 163°C .

Compound 2a: C, H analysis calcd for $\text{C}_{24}\text{H}_{56}\text{Mo}_3\text{O}_8\text{P}_4\text{Se}_{15}$: C 13.92; H 2.73. Found: C 14.18; H 2.89%. ^1H NMR (toluene- d_8 , δ , ppm): 1.14 (d, 6 Hz, 18H, CH_3), 1.15 (d, 6 Hz, 18H, CH_3), 1.18 (d, 6 Hz, 6H, CH_3), 1.19 (d, 6 Hz, 6H, CH_3), 4.77 (m, 6H, CH), 4.90 (m, 2H, CH); ^{31}P NMR (121.49 MHz, acetone- d_6 , δ , ppm): 61.2 (3P;

$J_{\text{P-Se}}$ 591, 607 Hz, $^3J_{\text{P-Se}}$ 52 Hz), 69.8 (1P; $J_{\text{P-Se}}$ 729 Hz), mp: 173 °C.

2.4. Syntheses of $[\text{Mo}_3(\mu_3\text{-Se})(\mu_2\text{-Se}_2)_3\{\text{Se}_2\text{P}(\text{O}i\text{-Pr})_2\}_3](X)$ ($X = \text{Cl}$, **2b**; Br , **2c**; I , **2d**)

The anion exchange reactions of **2a** with ammonium halides are very similar and only the representative experimental procedure of **2b** is listed below: Treatment of **2a** (20 mg, 0.01 mmol) with excess amount of NH_4Cl (50 mg, 0.94 mmol) in acetone (30 mL) for 6 h of stirring afforded red solution. After evaporation, the residue was subjected to column chromatography (silica gel) for purification (eluent: ethylacetate/*n*-hexane = 1/30). **2b** was obtained in 79% yield (13 mg). Good quality crystals for X-ray diffraction were grown from toluene.

Compound 2b: C, H analysis calcd for $\text{C}_{18}\text{H}_{42}\text{ClMo}_3\text{O}_6\text{P}_3\text{Se}_{13} \cdot \text{C}_7\text{H}_8$: C 15.89; H 2.65. Found: C 16.04; H 2.69%. ^1H NMR(300 MHz, CDCl_3 , δ , ppm): 1.30 (m, 36H, CH_3), 4.71 (m, 6H, CH); ^{31}P NMR (121.49 MHz, CDCl_3 , δ , ppm): 59.6 ($J_{\text{P-Se}}$ 590, 607 Hz, $^3J_{\text{P-Se}}$ 52 Hz); ^{77}Se NMR (95.38 MHz, CDCl_3 , δ , ppm): 261.1 (s, 3Se), 76.2 ($\mu_3\text{-Se}$), -95.2(s, 3Se), -93.5 (d, 3Se, $J_{\text{P-Se}}$ = 588), -125.7 (d, 3Se, $J_{\text{P-Se}}$ 608). Positive ion FAB-MS (Found/Calcd): m/z , 1761.5 (1762.9) [(M-Cl) $^+$]. mp: 165 °C.

Compound 2c: (64% yield, 17 mg) C, H analysis calcd for $\text{C}_{18}\text{H}_{42}\text{BrMo}_3\text{O}_6\text{P}_3\text{Se}_{13}$: C 11.71; H 2.28. Found: C 11.77; H 2.38%. mp: 169 °C.

Compound 2d: (70% yield, 19 mg) C, H analysis calcd for $\text{C}_{18}\text{H}_{42}\text{IMo}_3\text{O}_6\text{P}_3\text{Se}_{13} \cdot 1/2 \text{C}_6\text{H}_{14}$: C 13.06; H 2.56. Found: C 12.84; H 2.48%. mp: 171 °C.

2.5. X-ray structure determination

The structures of **1** and **2** were obtained by single crystal X-ray diffraction. Crystals were mounted on the tips of glass fibers with epoxy resin. Data for compounds **1** or **2** were collected on a SMART CCD (298(2) K) and a APEX II (293(2) K) diffractometers equipped with Mo $\text{K}\alpha$ radiation ($\lambda = 0.71073 \text{ \AA}$). Data reduction was performed with SAINT [16], which corrects for Lorentz and polarization effects. SADABS absorption correction was applied for compounds **2**. All structures were solved by the use of direct methods, and the refinement was performed by the least-squares methods on F^2 with the SHELXL-97 package [17], incorporated in SHELXTL/PC V5.10 [18]. Hydrogen atoms were added in idealized positions. Two independent molecules were identified in the asymmetric unit of structure **2a**. Selected crystal data for the compounds **1** and **2** are summarized in Table 1. Selected bond lengths (**1** and **2**), angles (**1**) and $\text{Se}\cdots\text{Se}$ and $\text{Se}\cdots\text{X}$ interactions (**2**) are listed in Table 2–4.

3. Results and discussion

3.1. Synthesis

The oxidized form of dsep ligands, $[(i\text{-PrO})_2\text{P}(\text{Se})\text{Se}]_2$, can be produced by either air oxidation [15a] or the addition of stoichiometric amount of I_2 into the acetone solution of $\text{KSe}_2\text{P}(\text{O}i\text{-Pr})_2$ [15b]. However, much higher yield and pure products of $[(i\text{-PrO})_2\text{P}(\text{Se})\text{Se}]_2$ can be prepared by utilizing FeCl_3 as the oxidant if the ammonium diisopropyl diselenophosphates [13f] were used. A large amount

Table 1
Crystallographic data for $[\text{Mo}_3(\mu_3\text{-Se})_4\{\text{Se}_2\text{P}(\text{O}i\text{-Pr})_2\}_6]$ (**1**), $[\text{Mo}_3(\mu_3\text{-Se})(\mu_2\text{-Se}_2)_3\{\text{Se}_2\text{P}(\text{O}i\text{-Pr})_2\}_3][\text{Se}_2\text{P}(\text{O}i\text{-Pr})_2]$ (**2a**), and $[\text{Mo}_3(\mu_3\text{-Se})(\mu_2\text{-Se}_2)_3\{\text{Se}_2\text{P}(\text{O}i\text{-Pr})_2\}_3](X)$ ($X = \text{Cl}$, **2b**; Br , **2c**; I , **2d**)

	1	2a	2b	2c	2d
Empirical formula	$\text{C}_{36}\text{H}_{84}\text{Mo}_4\text{O}_{12}\text{P}_6\text{Se}_{16}$	$\text{C}_{24}\text{H}_{56}\text{Mo}_3\text{O}_8\text{P}_4\text{Se}_{15}$	$\text{C}_{18}\text{H}_{42}\text{Mo}_3\text{O}_6\text{P}_3\text{Se}_{13}\text{Cl}$	$\text{C}_{18}\text{H}_{42}\text{Mo}_3\text{O}_6\text{P}_3\text{Se}_{13}\text{Br}$	$\text{C}_{18}\text{H}_{42}\text{Mo}_3\text{O}_6\text{P}_3\text{Se}_{13}\text{I}$
Molecular mass	2541.97	2068.79	1797.18	1841.64	1888.63
Temperature (K)	298(2)	293(2)	293(2)	293(2)	293(2)
Crystal system	Monoclinic	Monoclinic	Orthorhombic	Orthorhombic	Orthorhombic
Space group	$P2_1/n$	$P2_1/n$	$Pbca$	$Pbca$	$Pbca$
a (Å)	13.667(3)	25.0686(7)	14.9643(4)	15.180(2)	15.5412(6)
b (Å)	24.932(6)	8.8336(2)	23.6314(6)	23.757(4)	23.6688(9)
c (Å)	23.579(5)	52.4550(14)	26.5787(7)	26.279(4)	26.0514(10)
α (°)	90	90	90	90	90
β (°)	97.31(1)	100.7580(10)	90	90	90
γ (°)	90	90	90	90	90
V (Å ³)	7969(3)	11411.8(5)	9399.0(4)	9477(3)	9582.8(6)
Z	4	8	8	8	8
D_{calc} (Mg/m ³)	2.119	2.408	2.540	2.581	2.618
μ (Mo $\text{K}\alpha$) (mm ⁻¹)	8.085	10.365	11.045	11.741	11.422
Number of unique reflections	13554	20127	11671	8063	11469
R_{int}	0.0424	0.1277	0.0794	0.1047	0.1137
Number of reflections observed	13554	12493	7812	5264	7102
Final R indices [$I > 2\sigma(I)$]	$R_1^{\text{a}} = 0.0667$, $wR_2^{\text{b}} = 0.1372$	$R_1 = 0.0698$, $wR_2 = 0.1498$	$R_1 = 0.0332$, $wR_2 = 0.0594$	$R_1 = 0.0371$, $wR_2 = 0.0649$	$R_1 = 0.0335$, $wR_2 = 0.0572$

^a $R_1 = \sum ||F_o| - |F_c|| / \sum |F_o|$.

^b $wR_2 = \{ \sum [w(F_o^2 - F_c^2)]^2 / \sum [w(F_o^2)]^2 \}^{1/2}$.

Table 2
Selected bond lengths (Å) and angles (°) for $[\text{Mo}_4(\mu_3\text{-Se})_4\{\text{Se}_2\text{P}(\text{O}i\text{-Pr})_2\}_6]$ (1)

Mo(1)–Se(4)	2.458(2)	Mo(2)–Se(4)	2.461(2)
Mo(1)–Se(8)	2.466(2)	Mo(2)–Se(8)	2.466(2)
Mo(1)–Se(3)	2.482(2)	Mo(2)–Se(2)	2.503(2)
Mo(1)–Se(7)	2.696(2)	Mo(2)–Se(12)	2.692(2)
Mo(1)–Se(9)	2.704(2)	Mo(2)–Se(1)	2.702(2)
Mo(1)–Se(14)	2.729(2)	Mo(2)–Se(6)	2.721(2)
Mo(1)–Mo(2)	2.886(2)	Mo(2)–Mo(4)	2.934(2)
Mo(1)–Mo(3)	2.931(2)	Mo(2)–Mo(3)	2.936(2)
Mo(1)–Mo(4)	2.933(2)	Mo(3)–Se(16)	2.716(2)
Mo(3)–Se(2)	2.467(2)	Mo(3)–Mo(4)	2.822(2)
Mo(3)–Se(3)	2.469(2)	Mo(3)–Se(10)	2.696(2)
Mo(3)–Se(8)	2.497(2)	Mo(3)–Se(5)	2.701(2)
Mo(4)–Se(2)	2.458(2)	Mo(4)–Se(13)	2.691(2)
Mo(4)–Se(3)	2.468(2)	Mo(4)–Se(15)	2.692(2)
Mo(4)–Se(4)	2.499(2)	Mo(4)–Se(11)	2.729(2)
P(1)–Se(6)	2.156(5)	P(2)–Se(1)	2.161(4)
P(1)–Se(12)	2.156(5)	P(2)–Se(9)	2.149(4)
P(3)–Se(7)	2.152(4)	P(4)–Se(10)	2.173(4)
P(3)–Se(14)	2.161(4)	P(4)–Se(16)	2.133(5)
P(5)–Se(5)	2.165(4)	P(6)–Se(11)	2.134(4)
P(5)–Se(13)	2.145(4)	P(6)–Se(15)	2.165(4)
Se(4)–Mo(1)–Se(8)	106.45(6)	Se(4)–Mo(1)–Se(3)	104.72(6)
Se(8)–Mo(1)–Se(3)	104.72(6)	Se(4)–Mo(1)–Se(14)	161.93(7)
Se(8)–Mo(1)–Se(7)	162.52(7)	Se(3)–Mo(1)–Se(9)	158.14(6)
Se(7)–Mo(1)–Se(14)	79.08(5)	Se(9)–Mo(1)–Se(14)	82.19(6)
Se(7)–Mo(1)–Se(9)	77.56(5)	Se(4)–Mo(1)–Se(7)	85.35(6)
Se(3)–Mo(1)–Se(7)	84.03(6)	Se(3)–Mo(1)–Se(14)	82.86(6)
Se(8)–Mo(1)–Se(14)	86.92(6)	Se(4)–Mo(1)–Se(9)	85.58(6)
Se(8)–Mo(1)–Se(9)	90.30(6)	Mo(2)–Mo(1)–Mo(3)	60.61(4)
Mo(2)–Mo(1)–Mo(4)	60.56(4)	Mo(3)–Mo(1)–Mo(4)	57.54(4)
Mo(1)–Se(4)–Mo(2)	71.84(5)	Mo(2)–Se(4)–Mo(4)	72.54(5)
Mo(1)–Se(4)–Mo(4)	72.54(5)		

of orange-red crystals of bis(diisopropoxyselenophosphinoyl)diselenide, $[(i\text{-PrO})_2\text{P}(\text{Se})\text{Se}]_2$, whose structure comprises a Se_2 chain to bridge two $(i\text{-PrO})_2\text{P}(\text{Se})$ fragments [19], can be grown from diethyl ether solvent. The structure can also be delineated as two dsep units connected by a Se–Se bond.

Table 4
Intermolecular $\text{Se}\cdots\text{Se}$ and $\text{Se}\cdots\text{X}$ contacts (Å) of **2a–2d**

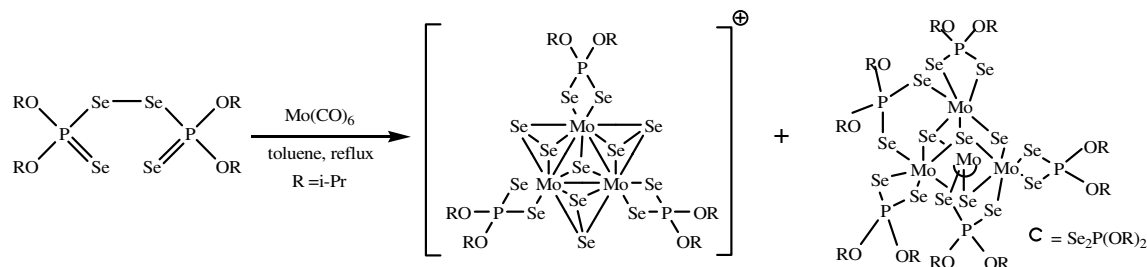
2a		2b		2c		2d	
Se3–Se6A	3.862	Cl1B–Se7	3.070	Br1I–Se2	3.879	I1E–Se2	4.054
Se6–Se13B	3.752	Cl1G–Se8	3.032	Br1I–Se7F	3.177	I1E–Se5	3.984
Se7–Se30A	3.597	Cl1B–Se9	3.000	Br1I–Se8	3.144	I1E–Se6F	3.301
Se8–Se29	3.699	Cl1B–Se12	2.801	Br1I–Se9F	3.134	I1E–Se9F	3.103
Se8–Se30	3.201	Se2–Se4E	3.625	Br1I–Se11F	2.927	I1E–Se10	3.291
Se9–Se30	3.032	Se2–Se7E	3.680	Se2–Se3F	3.673	I1E–Se11F	3.321
Se12–Se30	3.023	Se9–Se13F	3.716	Se2–Se7F	3.710	Se1F–Se5	3.731
Se16–Se19A	3.859			Se9F–Se13	3.820	Se5–Se11F	3.806
Se17–Se27C	3.664					Se6F–Se12	3.980
Se19–Se26B	3.733						
Se20–Se27C	3.791						
Se20–Se28C	3.225						
Se21–Se28D	3.646						
Se23–Se28C	3.044						
Se25–Se28C	3.025						

A: X, 1 + Y, Z. B: X, -1 + Y, Z. C: -1 + X, -1 + Y, Z. D: -1 + X, Y, Z. E: -1/2 + X, Y, 1/2 - Z. F: 1/2 + X, Y, 1/2 - Z. G: -1/2 + X, -1 + Y, 1/2 - Z. I: 1/2 + X, 1 + Y, 1/2 - Z.

Table 3
Selected bond lengths (Å) of **2a–2d**

	2a	2b	2c	2d
Mo–Mo	2.783(2) 2.784(2)	2.788(2)	2.788(2)	2.785(2)
	2.791(2) 2.791(2)	2.793(2)	2.798(2)	2.793(2)
	2.798(2) 2.792(2)	2.799(2)	2.804(2)	2.796(2)
Mo– μ_3 -Se	2.496(2) 2.495(2)	2.499(2)	2.499(2)	2.501(2)
	2.498(2) 2.495(2)	2.499(2)	2.504(2)	2.504(2)
	2.503(2) 2.503(2)	2.503(2)	2.504(2)	2.504(2)
Mo– Se_{eq}	2.594(2) 2.615(2)	2.614(2)	2.618(2)	2.612(2)
	2.618(2) 2.616(2)	2.616(2)	2.619(2)	2.616(2)
	2.619(2) 2.617(2)	2.616(2)	2.619(2)	2.619(2)
	2.620(2) 2.621(2)	2.617(2)	2.623(2)	2.621(2)
	2.621(2) 2.628(2)	2.619(2)	2.625(2)	2.623(2)
	2.635(2) 2.630(2)	2.625(2)	2.625(2)	2.625(2)
Mo– Se_{ax}	2.528(2) 2.530(2)	2.526(2)	2.533(2)	2.531(2)
	2.529(2) 2.531(2)	2.531(2)	2.535(2)	2.538(2)
	2.531(2) 2.533(2)	2.531(2)	2.538(2)	2.540(2)
	2.531(2) 2.537(2)	2.537(2)	2.541(2)	2.542(2)
	2.543(2) 2.537(2)	2.541(2)	2.545(2)	2.549(2)
	2.544(2) 2.539(2)	2.549(2)	2.551(2)	2.554(2)
Mo– Se_{cis}	2.657(2) 2.651(2)	2.646(2)	2.644(2)	2.647(2)
	2.659(2) 2.661(2)	2.648(2)	2.647(2)	2.648(2)
	2.663(2) 2.667(2)	2.648(2)	2.650(2)	2.655(2)
Mo– Se_{trans}	2.685(2) 2.684(2)	2.691(2)	2.691(2)	2.688(2)
	2.686(2) 2.687(2)	2.694(2)	2.696(2)	2.691(2)
	2.692(2) 2.689(2)	2.696(2)	2.699(2)	2.699(2)
$\text{Se}_{\text{eq}}\text{–Se}_{\text{ax}}$	2.314(2) 2.321(2)	2.310(2)	2.314(2)	2.315(2)
	2.319(2) 2.326(2)	2.320(2)	2.324(2)	2.333(2)
	2.336(3) 2.331(2)	2.328(2)	2.328(2)	2.333(2)

The oxidative decarbonylation of $\text{Mo}(\text{CO})_6$ with $[(i\text{-PrO})_2\text{P}(\text{Se})\text{Se}]_2$ in 2:3 molar ratio yielded two clusters $[\text{Mo}_4(\mu_3\text{-Se})_4\{\text{Se}_2\text{P}(\text{O}i\text{-Pr})_2\}_6]$ (**1**) (dark brown), and $[\text{Mo}_3(\mu_3\text{-Se})(\mu_2\text{-Se}_2)_3\{\text{Se}_2\text{P}(\text{O}i\text{-Pr})_2\}_3][\text{Se}_2\text{P}(\text{O}i\text{-Pr})_2]$ (**2a**) (orange) in ~50% and 25% yield, respectively (Scheme 1). When the molar ratio was 1:3, the tetranuclear cluster **1** was isolated in ~15% yield while **2a** in ~57% yield. The un-coordinated anion in **2a** can be replaced by the halide ions to afford $[\text{Mo}_3(\mu_3\text{-Se})(\mu_2\text{-Se}_2)_3\{\text{Se}_2\text{P}(\text{O}i\text{-Pr})_2\}_3](\text{X})$ (X = Cl, **2b**; Br, **2c**; I, **2d**) in 64–79% yield via the anion



Scheme 1.

exchange reactions of **2a** with ammonium halide in acetone. It is remarkable to note that the oxidative decarbonylation of $\text{Mo}(\text{CO})_6$ with the analogous sulfur ligands, $[\text{Et}_2\text{P}(\text{S})\text{S}]_2$ and $[(\text{EtO})_2\text{P}(\text{S})\text{S}]_2$, yielded only the trinuclear cluster, $[\text{Mo}_3\text{S}_7(\text{S}_2\text{PET}_2)_3][\text{S}_2\text{PET}_2]$ [20], and the tetranuclear cluster, $[\text{Mo}_4\text{S}_4\{\text{S}_2\text{P}(\text{OEt})_2\}_6]$ [21a], respectively. In contrast, both clusters, **1** and **2a**, were obtained from $[(i\text{-PrO})_2\text{P}(\text{Se})\text{Se}]_2$ and $\text{Mo}(\text{CO})_6$ in a one-pot reaction. Presumably the formation of **1** through the de-selenation of **2a** by the molybdenum was achieved and this hypothesis is sustained by the present study: the higher molar ratio of metal to ligand favors the higher yield of tetranuclear clusters. The ethyl derivative of **2c**, namely $[\text{Mo}_3(\mu_3\text{-Se})(\mu_2\text{-Se}_2)_3\{\text{Se}_2\text{P}(\text{OEt})_2\}_3](\text{Br})$ (**3**), was reported by Ibers and Berau [6]. However, it was synthesized by the selective substitution of bromo ligands in the material, $[\text{PPh}_4]_2\text{-}[\text{Mo}_3(\mu_3\text{-Se})(\mu_2\text{-Se}_2)_3\text{Br}_6]$ and the selenoorgano bidentate ligand, $\text{K}[\text{Se}_2\text{P}(\text{OEt})_2]$ [6].

Positive FAB-mass spectrum supports the formation of cluster **1**, with the molecular ion peak at $m/z = 2542.0$ ($M_{\text{calc}} = 2541.97$). Also observed are two fragment peaks at $m/z = 2233.4$ and 1926.5 , which correspond to the intact molecule with the loss of one ($M_{\text{calc}} = 2234.9$) and two dsep ligands ($M_{\text{calc}} = 1927.9$), respectively. Similarly, the cluster **2b** shows $[(\text{M}-\text{Cl})^+]$ at m/z , 1761.5, which is in good agreement with the calculated values of 1761.7.

3.2. Structures of **1** and **2**

Cluster **1** has a Mo_4Se_4 cubane-like core formed by triply bridging $\mu_3\text{-Se}$ atoms, and is surrounded by four chelating and two bridging dsep ligands, which are located on the opposite sides of the cube (Fig. 1). Thus each Mo atom is bonded to two Se atoms from one chelating dsep ligand, to one Se from a bridging dsep, and to three triply bridging $\mu_3\text{-Se}$ atoms. The $\text{Mo}-\mu_3\text{-Se}$ bonds (2.458(2)–2.503(2) Å) are comparable with 2.47(2) Å in $\text{Mo}_4(\mu_3\text{-Se})_4[\text{S}_2\text{P}(\text{OEt})_2]_6$ [7b], but shorter than the $\text{Mo}-(^1\eta\text{-Se})$ bond distances of the dsep ligands, 2.691(2)–2.729(2) Å. There are six Mo–Mo bonds: two bonds with distances at 2.822(2) and 2.886(2) Å ($\text{Mo}-\text{Mo}_{\text{bridging dsep}}$), and the other four in the range of 2.931(2)–2.936(2) Å ($\text{Mo}-\text{Mo}_{\text{chelating dsep}}$). The analogous Mo–Mo distances in $\text{Mo}_4(\mu_3\text{-Se})_4[\text{S}_2\text{P}(\text{OEt})_2]_6$ (α -form) [7b] are 2.754–2.781 and 3.002–3.025 Å, respectively. Therefore, the known “pulling together” effect of bridging ligands such as dithiophosphates, dithiocarba-

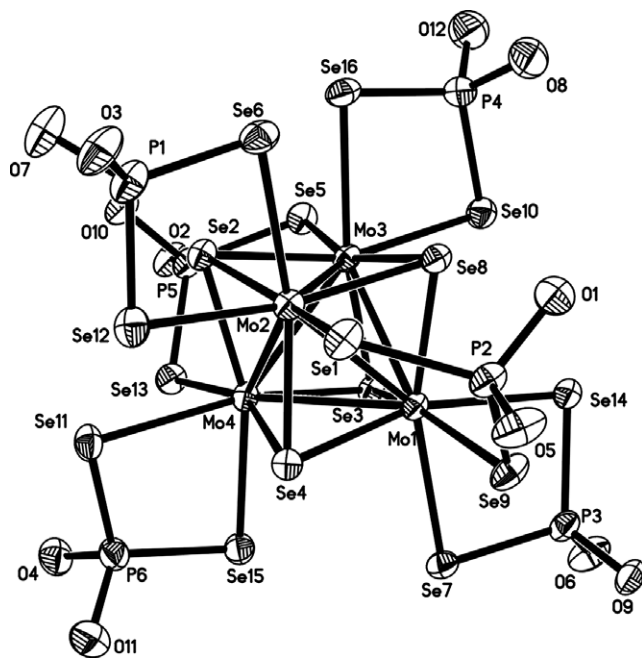


Fig. 1. Thermal ellipsoid drawing (50% probability) of the cluster, $\text{Mo}_4(\mu_3\text{-Se})_4[\text{Se}_2\text{P}(\text{O}i\text{-Pr})_2]_6$ (**1**) with isopropyl groups omitted for clarity.

mates, and acetates, regularly observed in complexes with the central Mo_4S_4 core [2,7b] also identified in the Mo_4Se_4 cuboidal core bridged by the dichalcophosphate ligands. The P–Se bonds in **1** lie in the range, 2.133(5)–2.165(4) Å, indicating a partial double bond character. The angles at the metal center (other than metal–metal bonds), for example, Mo1, vary in a wide range, ca. 77–163° with *trans* Se–Mo–Se angles being in the range, ca. 158–163°. The angles at triply bridging $\mu_3\text{-Se}$ center, Mo–Mo–Mo angles and Se–Mo–Se bite angles are ca. 72°, 60°, and 79°, respectively.

Theoretically a α -isomer of **1** which has three bridging and three chelating dsep ligands to surround the central Mo_4Se_4 core should exist in addition to the present β isomer. Surprisingly we can never identify the α -isomer either from the solution NMR measurement (vide infra) or the crystallographic study which is in sharp contrast to $\text{Mo}_4(\mu_3\text{-Se})_4[\text{S}_2\text{P}(\text{OEt})_2]_6$ in which the re-crystallization gave a mixture of α - and β -isomers [7b].

The general structural feature for the cluster cation in **2** has three Mo atoms in an equilateral triangle with Mo–Mo–Mo angle being, ca. 60° (Fig. 2). Mo–Mo distances

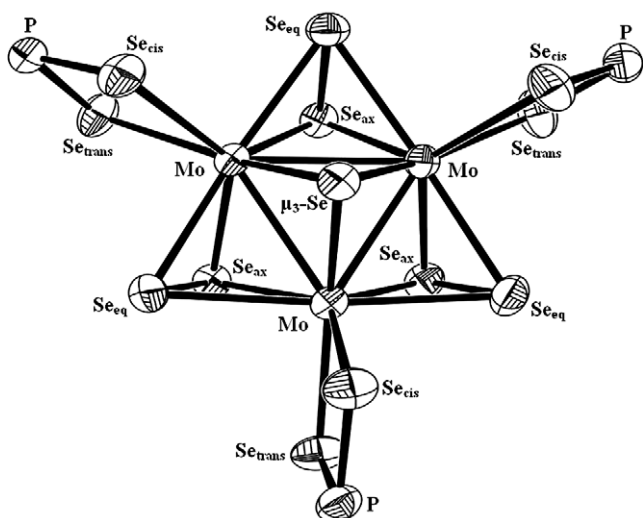


Fig. 2. Thermal ellipsoid drawing (50% probability) of the cluster cation, $[\text{Mo}_3(\mu_3\text{-Se})(\mu\text{-Se}_2)_3\{\text{Se}_2\text{P}(\text{O}i\text{-Pr})_2\}_3]^+$ (**2**) with isopropoxyl groups omitted for clarity.

lie in a close range, 2.783(2)–2.804(2) Å. These bond distances are very close to 2.783–2.790 Å in $[\text{Mo}_3(\mu_3\text{-Se})(\mu_2\text{-Se}_2)_3\{\text{Se}_2\text{P}(\text{OEt})_2\}_3](\text{Br})$ **3** [6]. The Mo_3 triangle is capped

by one apical $\mu_3\text{-Se}^{2-}$ ligand, and each side of the triangle is bridged by a $\mu_2\text{-Se}_2^{2-}$ group. Further $\mu_2\text{-Se}_2^{2-}$ ligands are non-symmetrically bonded to the Mo atoms. The Mo-Se_{ax} and Mo-Se_{eq} distances are 2.526(2)–2.554(2) and 2.594(2)–2.635(2) Å of which the Mo-Se_{eq} bond distances are always longer by about 0.1 Å. These distances are similar to ca. 2.554 and ca. 2.617 Å, respectively, in $[\text{Mo}_3(\mu_3\text{-Se})(\mu_2\text{-Se}_2)_3\{\text{Se}_2\text{P}(\text{OEt})_2\}_3](\text{Br})$ (**3**) [6]. The averaged $\text{Se}_{\text{eq}}\text{-Se}_{\text{ax}}$ distance is 2.323 Å, which is comparable with 2.321 Å in **3**. The $\text{Mo}-\mu_3\text{-Se}$ distances, 2.495(2)–2.504(2) Å, as well as $\text{Mo-Se}_{\text{cis}}$ (Av. 2.653 Å) and $\text{Mo-Se}_{\text{trans}}$ distances (Av. 2.691 Å) are similar to those in **3**. The $\text{Mo-Se}_{\text{cis}}$ bonds are always shorter than $\text{Mo-Se}_{\text{trans}}$ bonds and this is typical for all Mo_3Se_7 clusters [2]. Dsep ligands form four-membered rings via Se, Se-chelation with $\text{Se}_{\text{cis}}\text{-Mo-Se}_{\text{trans}}$ bite angle of 78.76°. The angles at the capping Se atom are, ca. 68°; while angles around each Mo atom vary in a wide range, 53–157°.

Weak intermolecular $\text{Se}\cdots\text{Se}$ interactions [22] which are shorter than 4.0 Å do exist between the adjacent Mo_3 units in **2a**. One of the Se atoms of the dsep ligand, Se6 (Se19 from the other independent Mo_3 unit), of one cluster displays interactions with both the capping, $\mu_3\text{-Se13B}$ ($\mu_3\text{-Se16B}$) atom and the Se3B (Se26B) atom of the dsep ligand

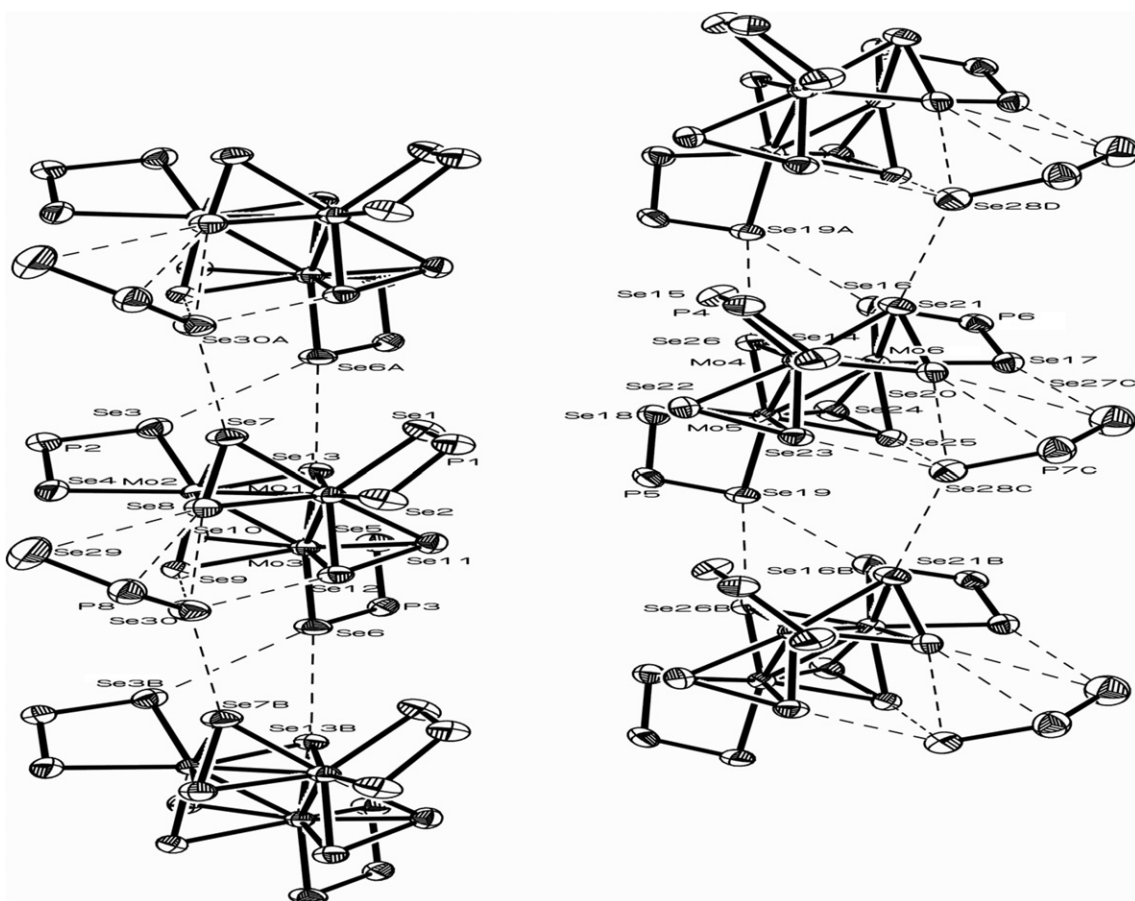


Fig. 3. Packing diagram of **2a** along the *c* direction displaying secondary $\text{Se}\cdots\text{Se}$ interactions with isopropoxyl groups omitted for clarity. Symmetry codes: A = $X, 1 + Y, Z$; B = $X, -1 + Y, Z$; C = $-1 + X, -1 + Y, Z$; D = $-1 + X, Y, Z$.

of the neighboring Mo_3 unit to produce infinite chain as depicted in Fig. 3. In addition, both Se atoms of the anion show contacts with Se atoms of the cluster cations. For example, Se28C interacts with three electrophilic, Se_{ax} atoms (Se20, Se23, and Se25) of the Mo_3 unit, and one equatorial Se21B atom of the adjacent Mo_3 unit. The other Se atom of the uncoordinated anion, Se27C, interacts with Se17 atom of the chelating, dsep ligand and electrophilic Se20 atom. Also observed is the presence of weak interactions between the diselenophosphate phosphorus and a selenium atom on one of the clusters which might be imposed by the $\text{Se}\cdots\text{Se}$ contacts.

A different, intermolecular $\text{Se}\cdots\text{Se}$ connecting pattern which yields the infinite chain was uncovered when the uncoordinated dsep anions were substituted to halides. Instead of the interaction between one Se atom of the dsep ligand of one cluster and the capping Se atom of the neighboring unit, here the contact exists in one of the electrophilic, axial Se atoms. Besides, the apical, μ_3 -Se13 atom also exhibits an interaction with Se9E atom (axial) of the adjacent Mo_3 unit. Furthermore, chloride shows interactions with three Se_{ax} atoms: Se7, Se9 and Se12 and one equatorial Se8 atom of the neighboring Mo_3 unit. The $\text{Se}\cdots\text{Se}$ interactions lie in the range, 3.625–3.716 Å, while

$\text{Cl}\cdots\text{Se}$ interactions lie in the range, 2.801–3.070 Å, which are less than the sum of van der Waals radii {4.0 Å, Se, Se; Cl, Se, 3.80 Å} [23]. A packing diagram depicting those $\text{Se}\cdots\text{Se}$ and $\text{Se}\cdots\text{Cl}$ interactions is displayed in Fig. 4a.

Though cluster **2c** is similar to $[\text{Mo}_3(\mu_3\text{-Se})(\mu_2\text{-Se}_2)_3\{\text{Se}_2\text{P}(\text{OEt})_2\}_3]\text{Br}$ (**3**) [6], yet these differ in the sense that the former exhibited unusual, secondary $\text{Se}\cdots\text{Se}$ interactions to form infinite chains. A packing diagram exhibiting those $\text{Se}\cdots\text{Se}$ and $\text{Se}\cdots\text{Br}$ interactions is displayed in Fig. 4b. It may be attributed to the effect of different substituents in two cases. The $\text{Se}\cdots\text{Se}$ interactions lie in the range, 3.673–3.820 Å. The $\text{Br}\cdots\text{Se}$ interactions lie in the range, 2.927–3.879 Å, which are shorter than the sum of van der Waals radii of Br^- and Se^{2-} (3.94 Å) [23].

Like **2b** and **2c**, iodide shows interactions with three electrophilic Se_{ax} atoms and one equatorial Se10 atom from the adjacent Mo_3 unit. The iodide further displays weak secondary interactions, 4.054 and 3.984 Å, with two Se atoms from two dsep ligands of the second Mo_3 molecule (Fig. 4c). The longest $\text{Se}\cdots\text{Se}$ distance of 3.980 Å, which approaches the upper limit of the secondary interaction, is observed between the capping Se12 atom and the axial Se6F atom of the adjacent unit. The $\text{Se}\cdots\text{Se}$ interactions lie in the range, 3.731–3.806 Å, while $\text{I}\cdots\text{Se}$ interac-

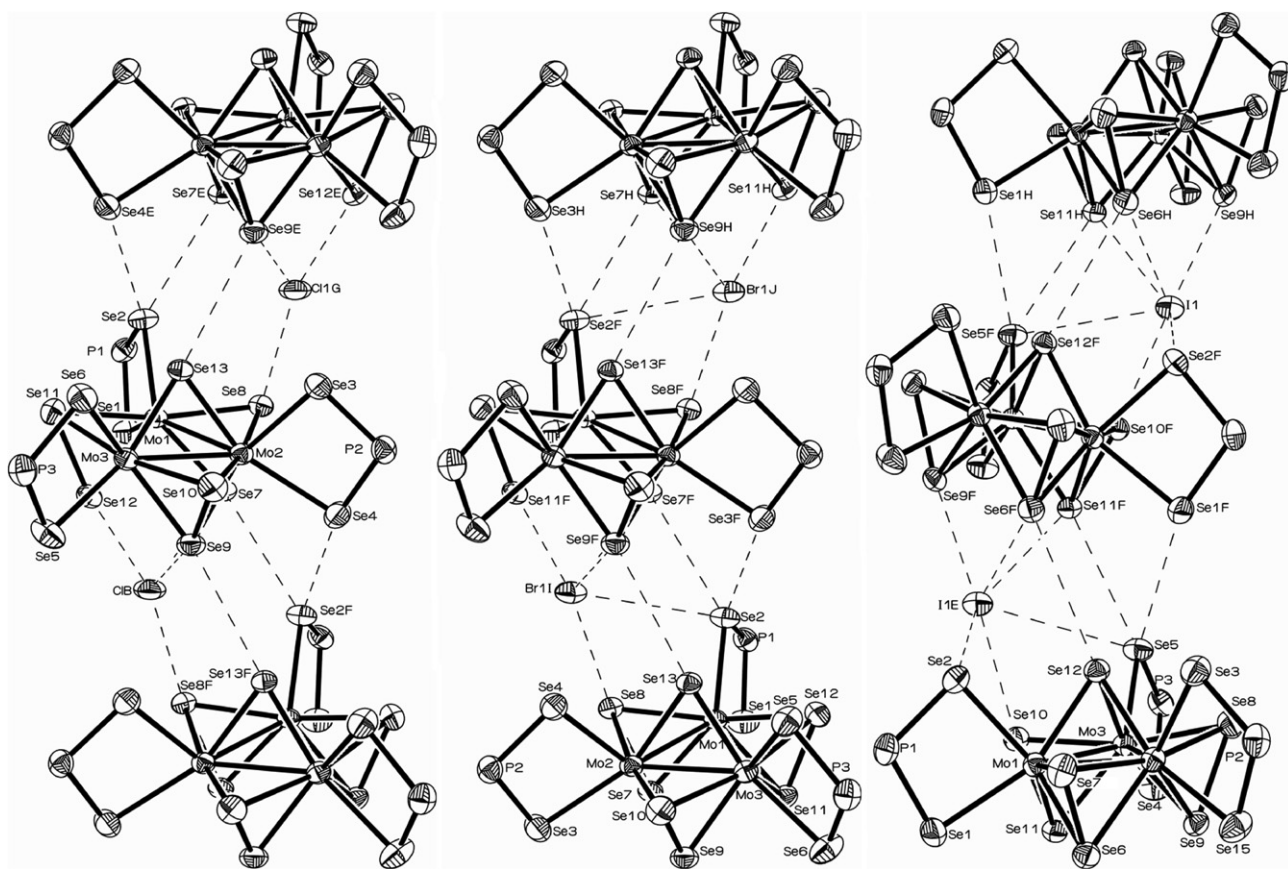


Fig. 4. (Left) Packing diagram of **2b** along the *b* direction displaying $\text{Se}\cdots\text{Se}$ and $\text{Se}\cdots\text{X}$ interactions with isopropoxyl groups omitted; (middle) **2c**; (right) **2d**. Symmetry codes: B = X, $-1 + Y, Z$; E = $-1/2 + X, Y, 1/2 - Z$; F = $1/2 + X, Y, 1/2 - Z$; G = $-1/2 + X, -1 + Y, 1/2 - Z$; H = $1 + X, Y, Z$; I = $1/2 + X, 1 + Y, 1/2 - Z$; J = $1 + X, 1 + Y, Z$.

tions lie in the range, 3.103–4.054 Å, which are less than the sum of van der Waals radii (I, Se, 4.15 Å) [23].

It is interesting to note that in the crystal packing the halides are sandwiched between clusters in both sides along the molecular axis while the dsep anions are identified only in one side. Besides, intermolecular, secondary Se–Se interactions can be found between Se atoms of the adjacent dsep ligands and one Se atom of the dsep to one Se_{ax} atom of the neighboring unit to generate the infinite chain in **2b–2d**. All halides are attached to three Se_{ax} and one Se_{eq} atoms and these distances are far shorter than the sum of the van der Waals radii. Surprisingly, this sort of contacts is different to their sulfur analog where the interaction between the equatorial S atom and halide donor atom was never identified [2]. Hence secondary, weak $\text{Se}\cdots\text{Se}$ and $\text{Se}\cdots\text{X}$ interactions must be added into the list of non-covalent interactions essential for specific packing and supramolecular aggregation. Previously weak, $\text{Se}\cdots\text{Se}$ interactions of the dsep ligands from the neighboring molecules has yielded to dimer formation in neutral, tris-chelated compounds of the type, $\text{In}[\text{Se}_2\text{P}(\text{OR})_2]_3$ [24].

3.3. NMR spectroscopy and electrochemistry

The ^{31}P NMR spectrum of cluster **1** exhibits two singlets flanked with selenium satellites at 120.7 and 85.1 ppm which correspond to the chelating and bridging *dsepl* ligands, respectively, the ratio of integrated intensities being 2:1 and in good agreement with the structural study. Similarly, ^{77}Se NMR showed signals due to $\mu_3\text{-Se}$, as well as bridging and chelating *dsep* ligands at δ values of 126.3, 38.0, and –35.1 ppm, respectively. Thus β -isomers which have two bridging and four chelating ligands form exclusively in solution in this case. The ^1H NMR spectrum of **1** displayed three doublets and three multiplets, which chemical shifts are listed in the experimental section and correspond to the methyl and methine protons of the isopropyl groups. The integration ratio of each doublet is 1:1:1, so is each multiplet. Apparently three different types of isopropyl group exist: one is connected to O atoms of the bridging dsep ligands, the other is the inner O atoms (O6, O7, O8, O11) in the chelating dsep ligands, another is the outer O atoms (O3, O4, O9, O12). The latter two types can not be interchanged by any symmetry elements. Hence three signals of isopropyl group are consistent with this structure.

The ^{31}P chemical shift of the anionic dsep ligand in **2a** appeared at 69.8 ppm which shows an upfield shift relative to its ammonium salt (81 ppm) [13f]. The δ value of three, coordinated dsep ligands is at 61.2 ppm and is flanked with two sets of selenium satellites. The three P atoms are equivalent by symmetry in the solid state, which is maintained in solution and thus only one signal is observed. Two sets of selenium satellites are reminiscent of two Se atoms (Se_{cis} and Se_{trans}) of the dsep ligand relative to the capping, $\mu_3\text{-Se}$ (Se13) atom. In addition, the $^3J_{\text{P-Se}}$ coupling is also observed. The ^{31}P NMR spectrum of cluster **2b** exhibited

one signal at $\delta_{\text{P}} = 59.6$ ppm. In the ^{77}Se NMR spectrum, three types of Se atoms within the $[\text{Mo}_3(\mu_3\text{-Se})(\mu_2\text{-Se}_2)_3]^{4+}$ core and the two Se atoms (Se_{cis} and Se_{trans}) of the dsep ligand were observed. The peak with the smallest intensity, $\delta 76.2$ ppm, can be assigned to the capping $\mu_3\text{-Se}^{2-}$ atom which is close to 76.9 ppm for cluster **3** [6]. Two Se atoms of the bridging ligand, Se_2^{2-} , are readily observed at 261.2 and –95.2 ppm, respectively. The remaining two doublets, –93.5 ($J_{\text{P-Se}} = 588$ Hz) and –125.7 ($J_{\text{P-Se}} = 608$ Hz), are the characteristics of the dsep ligand.

The electron transfer properties of the tetra-molybdenum cluster, **1**, were studied by cyclic voltammetric techniques in CH_2Cl_2 solvent at 25 °C. The cyclic voltammogram of **1** in CH_2Cl_2 -0.1 M TBAHP reveals quasi-reversible voltammograms at 0.67, –0.23, and –1.09 V vs Ag/AgCl, at a scan rate of 50 mV s^{-1} . Since the oxidation state of the Mo atoms in $\text{Mo}_4\text{Se}_4^{6+}$ are described as formally two Mo(IV) and two Mo(III), thus the quasi-reversible one-electron oxidation wave ($E_{1/2} = 0.67$ V) corresponds to the formation of the $\text{Mo}_4\text{Se}_4^{7+}$ state, and two quasi-reversible one-electron reduction waves ($E_{1/2} = -0.23$ and –1.09 V) suggest the formation of $\text{Mo}_4\text{Se}_4^{5+}$ and $\text{Mo}_4\text{Se}_4^{4+}$ cores.

Acknowledgment

Financial support from the National Science Council of Taiwan (NSC 95-2119-M-259-001) is greatly acknowledged.

Appendix A. Supplementary data

CCDC 623099, 623100, 623101, 623102 and 623103 contain the supplementary crystallographic data for **1**, **2a**, **2b**, **2c** and **2d**. These data can be obtained free of charge via <http://www.ccdc.cam.ac.uk/conts/retrieving.html>, or from the Cambridge Crystallographic Data Centre, 12 Union Road, Cambridge CB2 1EZ, UK; fax: (+44) 1223-336-033; or e-mail: deposit@ccdc.cam.ac.uk. Supplementary data associated with this article can be found, in the online version, at doi:10.1016/j.jorganchem.2006.12.034.

References

- [1] (a) R. Llusar, S. Uriel, C. Vicent, J.M. Clemente-Juan, E. Coronado, C.J. Gomez-Garcia, B. Braida, E. Canadell, *J. Am. Chem. Soc.* 126 (2004) 12076; (b) R. Llusar, S. Triguero, S. Uriel, C. Vicent, E. Coronado, C.J. Gomez-Garcia, *Inorg. Chem.* 44 (2005) 1563.
- [2] M.N. Sokolov, V.P. Fedin, A.G. Sykes, in: J.A. McCleverty, T.J. Meyers (Eds.), *Comprehensive Coordination Chemistry II*, vol. 4, Elsevier, New York, 2003, pp. 768–824.
- [3] V.P. Fedin, G.J. Lamprecht, T. Kohzuma, W. Clegg, M.R.J. Elsegood, A.G. Sykes, *J. Chem. Soc., Dalton Trans.* (1997) 1747.
- [4] (a) D.M. Saysell, V.P. Fedin, G.J. Lamprecht, M.N. Sokolov, A.G. Sykes, *Inorg. Chem.* 36 (1997) 2982;

- (b) R. Hernandez-Molina, D.N. Dybtsev, V.P. Fedin, M.R.J. Elsegood, W. Clegg, A.G. Sykes, *Inorg. Chem.* 37 (1998) 2995.
- [5] V.P. Fedin, M.N. Sokolov, K.G. Myakishev, O.A. Geras'ko, V.Y. Fedorov, *Polyhedron* 10 (1991) 1311.
- [6] V. Berau, J.A. Ibers, *C. R. Acad. Sci., Ser. IIC: Chim.* 3 (2000) 123.
- [7] (a) M.N. Sokolov, A.L. Gushchin, D.Yu. Naumov, O.A. Gerasko, V.P. Fedin, *Inorg. Chem.* 44 (2005) 2431;
(b) M.N. Sokolov, P. Esparza, R. Hernandez-Molina, J.G. Platas, A. Mederos, J.A. Gavin, R. Llusar, C. Vicent, *Inorg. Chem.* 44 (2005) 1132.
- [8] C. Magliocchi, X. Xie, T. Hughbanks, *Inorg. Chem.* 43 (2004) 1902.
- [9] (a) G. Henkel, G. Kampmann, B. Krebs, G.J. Lamprecht, M. Nasreldin, A.G. Sykes, *Chem. Commun.* (1990) 1014;
(b) M. Nasreldin, G. Henkel, G. Kampmann, B. Krebs, G.J. Lamprecht, C.A. Routledge, A.G. Sykes, *J. Chem. Soc., Dalton Trans.* (1993) 737.
- [10] W. McFarlane, M. Nasreldin, D.M. Saysell, Z.-S. Jia, W. Clegg, M.R.J. Elsegood, K.S. Murray, B. Moubaraki, A.G. Sykes, *J. Chem. Soc., Dalton Trans.* (1996) 363.
- [11] P. Baird, J.A. Bandy, M.L.H. Green, A. Hamnett, E. Marseglia, D.S. Obertelli, K. Prout, J. Qin, *J. Chem. Soc., Dalton Trans.* (1991) 2377.
- [12] Q.-F. Zhang, Y.-N. Xiong, T.-S. Lai, W. Ji, X.-Q. Xin, *J. Phys. Chem. B* 104 (2000) 3446.
- [13] (a) C.W. Liu, H.-C. Chen, J.-C. Wang, T.-C. Keng, *Chem. Commun.* (1998) 1831;
(b) C.W. Liu, C.-M. Hung, J.-C. Wang, T.-C. Keng, *J. Chem. Soc., Dalton Trans.* (2002) 3482;
(c) C.W. Liu, C.-M. Hung, B.K. Santra, Y.-H. Chu, Z. Lin, *Inorg. Chem.* 43 (2004) 4306;
(d) C.W. Liu, C.-M. Hung, H.-C. Chen, J.-C. Wang, T.-C. Keng, K.-M. Guo, *Chem. Commun.* (2000) 1897;
(e) C.W. Liu, I.-J. Shang, J.-C. Wang, T.-C. Keng, *Chem. Commun.* (1999) 995;
- (f) C.W. Liu, I.-J. Shang, C.-M. Hung, J.-C. Wang, T.-C. Keng, *J. Chem. Soc., Dalton Trans.* (2002) 1974;
- (g) B.K. Santra, C.-M. Hung, B.-J. Liaw, J.-C. Wang, C.W. Liu, *Inorg. Chem.* 43 (2004) 7570;
- (h) C.W. Liu, I.-J. Shang, R.-J. Fu, B.-J. Liaw, J.-C. Wang, I.-J. Chang, *Inorg. Chem.* 45 (2006) 2335;
- (i) C.W. Liu, T.S. Lobana, B.K. Santra, C.-M. Hung, H.-Y. Liu, B.-J. Liaw, J.-C. Wang, *Dalton Trans.* (2006) 560.
- [14] (a) C.W. Liu, Phosphorus, Sulfur Silicon Relat. Elem. 180 (2005) 923;
(b) T.S. Lobana, J.-C. Wang, C.W. Liu, *Coord. Chem. Rev.* 251 (2007) 91.
- [15] (a) M.V. Kudchadker, R.A. Zingaro, K.J. Irgolic, *Can. J. Chem.* 46 (1968) 1415;
(b) R.D. Gorak, N.I. Zemlyanskii, *Z. Obsh. Khim.* 41 (1971) 1994.
- [16] SAINT V4.043: Software for the CCD Detector System, Bruker Analytical X-ray System, Madison, WI, 1995.
- [17] G.M. Sheldrick, *SHELXL-97: Program for the Refinement of Crystal Structure*, University of Göttingen, Göttingen, Germany, 1997.
- [18] *SHELXL 5.10 (PC Version)*, Program Library for Structure Solution and Molecular Graphics, Bruker Analytical X-ray System, Madison, WI, 1998.
- [19] V. Berau, J.A. Ibers, *Acta Crystallogr., Sect. C* 56 (2000) 584.
- [20] (a) H. Keck, W. Kuchen, J. Mathow, *Inorg. Synth.* 23 (1985) 118;
(b) I. Haiduc, L.Y. Goh, *Coord. Chem. Rev.* 224 (2002) 151.
- [21] (a) C.L. Coyle, K.A. Eriksen, S. Farina, J. Francis, Y. Gea, M.A. Greaney, P.J. Guzi, T.R. Halbert, H.H. Murray, E.I. Stiefel, *Inorg. Chim. Acta* 198 (1992) 565;
(b) T.C.W. Mak, K.S. Jasim, C. Chieh, *Inorg. Chem.* 24 (1985) 1587.
- [22] R. Gleiter, D.B. Werz, B.J. Rausch, *Chem. Eur. J.* 9 (2003) 2677.
- [23] N.A. Lange, *Lange's Handbook of Chemistry*, 11th ed., McGraw-Hill, New York, 1973.
- [24] J.-M. Chen, B.K. Santra, C.W. Liu, *Inorg. Chem. Commun.* 7 (2004) 1103.